Aeroelastic analysis through linear and non-linear methods: a summary of flutter prediction in the PUMA DARP

N. V. Taylor, C. B. Allen, A. L. Gaitonde, D. P. Jones
University of Bristol

G. A . Vio, J. E. Cooper
University of Manchester

A. M. Rampurawala, K. J. Badcock, M. A. Woodgate
University of Glasgow

M. J. de C. Henshaw
BAE Systems

ABSTRACT

This paper presents a comparison of linear and non-linear methods for the analysis of aeroelastic behaviour and flutter boundary prediction. The methods in question include NASTRAN and ZAERO, based on linear aerodynamics, and the non-linear coupled CFD-CSD methods RANSMB and PMB, developed at the Universities of Bristol and Glasgow respectively. The test cases used for this comparison are the MDO and AGARD 445.6 weakened wing. In general, it was found that the non-linear methods demonstrate excellent agreement with respect to pressure distributions, deflections, dynamic behaviour, and flutter boundary locations for both cases. This is in contrast to previous studies involving similar methods, where notable differences across the MDO span were found, and is taken to imply good performance of the CFD-CSD interpolation schemes employed here. While the linear methods produce similar flutter boundaries to the coupled codes for the aerodynamically simple AGARD 445.6 wing, results for the transonic 'rooftop' MDO wing design did not agree as well.

NOMENCLATURE

a	damping coefficient of stiffness matrix
b	damping coefficient of mass matrix
$\mathbf{C}$	damping matrix
E	total energy
f_a	aerodynamic force vector acting on aerodynamic grid
f_s	aerodynamic force vector acting on structural grid
$\mathbf{F}, \mathbf{G}, \mathbf{H}$	flux vector in x, y, z
$\mathbf{G_{as}}$	interpolation matrix
$\mathbf{K}$	stiffness matrix
$\mathbf{M}$	mass matrix
p	pressure
$\mathbf{R}$	residual vector
$\mathbf{S}$	spline matrix
t	time
u, v, w	velocity components in x, y, z
$\bar{U}, \bar{V}, \bar{W}$	contravariant velocity components in x, y, z
V	cell volume
$\mathbf{W}$	vector of conserved variables
x_a	aerodynamic surface grid point
x_s	structural surface grid point
x, y, z	Cartesian co-ordinates
α	vector of modal displacements
ϕ	mode vector
ψ	grid motion blending function.
ρ	density
ω	modal (natural) frequency
ζ	damping ratio

Paper No. 2945. Manuscript received 14 October 2004, revised version received 19 October 2005, accepted 12 December 2005.

https://doi.org/10.1017/S0001924000013208 Published online by Cambridge University Press

INTRODUCTION

The prediction of flutter is an important area of aircraft design. Methods currently common in industry for this purpose involve the use of linear techniques, allowing uncoupling of the aerodynamic and structural equations. However, this reduces the accuracy of the methods, as real flows of practical interest are often non-linear in nature (particularly transonic flight). As flutter must be avoided at all costs, this leads to the need for significant safety margins, creating over-stiff and hence high mass designs. More significantly, it is likely that any errors in design will only be identified during flight testing. This extends the length of the flight test programme (typically at a cost of thousands of dollars an hour), as a lack of confidence in the prediction means that the initial tests must be carried out well below the expected onset of the unstable behaviour, and speed increased only gradually. Further, the cost of fixing any errors encountered at this stage is considerably greater than would be the case if they were to be identified before prototype manufacture through accurate modelling.

Prediction methods proven to be of greater accuracy will therefore lead directly to significant cost savings, without requiring any advances in the underlying aerodynamic or structural design methods. Even simulation tools with computational overheads too great to be used during the design process will produce notable savings, as their use will allow a reduction in the flight test programme. For this reason, the aeroelastics group within the PUMA (Progress in Unsteady Modelling of Aerodynamics) DARP (Defence Aerospace Research Partnership) set up in 2003 has been tasked with developing and comparing both more advanced 'fast flutter' analysis methods for use in the design loop, and time-domain simulation tools. This paper highlights some of the early work undertaken for the project, concentrating primarily on the simulation tools. The focus is on two key areas; the mesh motion and dynamic simulation produced by the time domain methods, known from previous work to be an area where differing results may be produced even from superficially similar schemes, and a comparison with linear based techniques in an effort to demonstrate when and where the more computationally intensive techniques are necessary, and when simpler methods are sufficient.

2.0 DESCRIPTION OF CFD CODES

2.1 Aerodynamic formulation and solution

Although both PMB and RANSMB are capable of Navier-Stokes solutions, such are currently prohibitively time consuming for three dimensional unsteady analysis. For this reason, only the Euler equations were solved. These may be written in non-dimensional conservative form as

$$\frac{\partial W}{\partial t}+\frac{\partial F}{\partial x}+\frac{\partial G}{\partial y}+\frac{\partial H}{\partial z}=0 \qquad \ldots (1)$$

where $\mathbf{W} = (\rho, \rho u, \rho v, \rho w, \rho E)^T$ denotes the vector of conserved variables. The flux vectors **F**, **G** and **H** are,

$$\mathbf{F}=\begin{pmatrix}\rho\bar{U}\\ \rho u\bar{U}+p\\ \rho v\bar{U}\\ \rho w\bar{U}\\ \bar{U}(\rho E+p)+x_t p\end{pmatrix},\mathbf{G}=\begin{pmatrix}\rho\bar{V}\\ \rho u\bar{V}\\ \rho v\bar{V}+p\\ \rho w\bar{V}\\ \bar{V}(\rho E+p)+y_t p\end{pmatrix}, \qquad \ldots (2)$$

$$\mathbf{H}=\begin{pmatrix}\rho\bar{W}\\ \rho u\bar{W}\\ \rho v\bar{W}\\ \rho w\bar{W}+p\\ \bar{W}(\rho E+p)+z_t p\end{pmatrix}$$

In the above ρ, u, v, w, p and E denote the density, the three Cartesian components of the velocity, pressure, and the specific total energy respectively. The terms $\bar{U}$, $\bar{V}$, $\bar{W}$ are the contravariant velocities defined by

$$\bar{U}=u-x_t,\bar{V}=v-y_t,\bar{W}=w-z_t \qquad \ldots (3)$$

where x_t, y_t, and z_t are the grid speeds in the Cartesian directions.

The Euler equations are discretised using the two codes described below on curvilinear multi-block body conforming grids using a cell-centred finite volume method which converts the partial differential Equations (1) into a set of ordinary differential equations which may be written as

$$\frac{\mathrm{d}}{\mathrm{d}t}\left(V_{i,j,k}W_{i,j,k}\right)=-R_{i,j,k}(W) \qquad \ldots (4)$$

Solution in the University of Glasgow code PMB (Parallel MultiBlock) is through an upwind implicit method based on that of Osher[1]. MUSCL variable extrapolation[2] is used to provide second-order accuracy with the Van Albada limiter to prevent spurious oscillations around shock waves. The time derivative is approximated by a second-order backwards derivative[3]. The University of Bristol has extended the BAE Systems code RANSMB (Reynolds Averaged Navier-Stokes MultiBlock), a cell centred finite volume solver of a Jameson type[4], to allow fully implicit unsteady calculations through pseudo-time stepping[3,5]. Convergence in the time domain occurs through a modified Runga-Kutta scheme due to Melson[6].

2.2 Structural modelling

In all cases reported here the structural behaviour was modelled using a modal approximation derived from the commercial FE package MSC NASTRAN. Mode shapes and frequencies are derived by solving the equation

$$\left[K-\omega_i^2 M\right]\phi_i=0 \qquad \ldots (5)$$

where ϕ_i are the mode shape vectors and ω_i the frequencies.

Introducing an arbitrary level of damping [**C**], defined following Ref. 7 by

$$[C]=a[K]+b[M] \qquad \ldots (6)$$

into the system allows more rapid attainment of steady state deflections under stable flow conditions, as well as allowing steady state responses beyond the flutter boundary to be determined. It also allows analysis of the actual effects of realistic structural damping on models, where damping behaviour is known. The equation of motion of the structure may then be expressed as

$$[\mathbf{M}]\delta\ddot{x}_s+[\mathbf{C}]\delta\dot{x}_s+[\mathbf{K}]\delta x_s=f_s \qquad \ldots (7)$$

where $\boldsymbol{\delta x_s}$ is a vector of displacements on a grid of points x_s, and f_s is the external force. If the structural motion is assumed linear (and hence [**M**], [**C**], and [**K**] are constant for a given structure), this equation may be solved either by modal analysis, or by direct integration of [**M**], [**C**], and [**K**].

https://doi.org/10.1017/S0001924000013208 Published online by Cambridge University Press

2.3 Modal equations

The modal output is non-dimensionalised with respect to mass such that

$$\phi_i^T [M] \phi_i = 1 \quad \ldots (8)$$

Using this approach results in a modal version of Equation (6):

$$\ddot{\alpha} + 2\omega\zeta\dot{\alpha} + \omega^2\alpha = [\phi] f_s \quad \ldots (9)$$

where $\boldsymbol{\omega}$ is the vector of mode frequency, $\boldsymbol{\zeta}$ that of damping ratio, $\boldsymbol{\alpha}$ the vector of modal displacements, and $[\boldsymbol{\phi}]$ the matrix composed of the mode shape vectors $\boldsymbol{\phi}$. The value of the damping ratio follows from the specification of a and b in Equation (5) via

$$\zeta_i = \frac{1}{2}\left(a\omega_i + \frac{b}{\omega_i} \right) \quad \ldots (10)$$

and may either be selected to best represent the damping behaviour of a real wing or, if artificial damping is intended, ζ_i itself may be directly specified to give the desired characteristics. Once the modal displacement is calculated, the Cartesian displacement at each node follows from

$$\delta x_s = [\phi]\alpha \quad \ldots (11)$$

These equations are solved using a Runga-Kutta approach in PMB, and a Newmark scheme in RANSMB[8]. Strong coupling is used to avoid introducing sequencing errors and phase lags. In both codes, the formulation is such that time step size may be selected on the basis of the model dynamics rather than any CFD or coupling considerations.

2.4 Inter-grid transfer

The aerodynamic forces are calculated at face centres on the aerodynamic surface grid. The problem of communicating these forces to the structural grid and returning the structural deflections to the fluid surface grid is complicated in the common situation that these grids not only do not match, but are also not even defined on the same surface. Denoting the fluid surface grid locations and aerodynamic forces as x_a and f_a, then a linear relationship to the corresponding structural values is used in the form

$$\delta x_a = \mathbf{S}(x_a, x_s) x_s \quad \ldots (12)$$

and then by the principle of virtual work, $f_s = \mathbf{S}^T f_a$. The matrix $\mathbf{S}$ is called the spline matrix.

The grid speeds on the wing surface are also needed and these are approximated directly from the transformation as

$$\delta\dot{x}_a = \mathbf{S}(x_a, x_s)\delta\dot{x}_s \quad \ldots (13)$$

where the structural grid speeds are given by

$$\delta\dot{x}_s = \sum \dot{\alpha}_i \phi_i \quad \ldots (14)$$

Both solvers make use of the CVT (constant volume tetrahedra) approach due to Goura[9], in linear form. In PMB each aerodynamic point is assigned a tetrahedra, and the tetrahedra equations are linearised at each time step. RANSMB makes use of an intermediate plane formed by the intersection of the outward normals of the structural grid and the aerodynamic surface. The motion of this intermediate grid is derived through consideration of CVTs formed between it and the structural mesh, and the TPS (thin plate spline) method is then used to interpolate from the intermediate grid to the aerodynamic surface[10].

2.5 Volume grid movement

Both codes interpolate volume grid points x_{ijk} as

$$\delta x_{ijk} = \phi_j^0 \delta x_{a\,jk} \quad \ldots (15)$$

where ψ_j^0 are values of a blending function[11] which varies between one at the wing surface (here j = 1) and zero at the block face opposite. The surface deflections $x_{a,\,ik}$ are obtained from the transformation of the deflections on the structural grid and so ultimately depend on the values of α_i. In PMB block sides internal to the flow or on other types of boundaries are fixed, whereas RANSMB employs a sprung block system.

Cell volumes are recalculated using a global conservation law by considering volume fluxes through cell sides. In the present calculations the geometric conservation law (GCL) was used. The input for the grid movement method is therefore the change in the point locations and velocities on the wing surface from the last time the volume grid vertex locations and speeds were calculated. This information is obtained from the structural solution through the transformation described above.

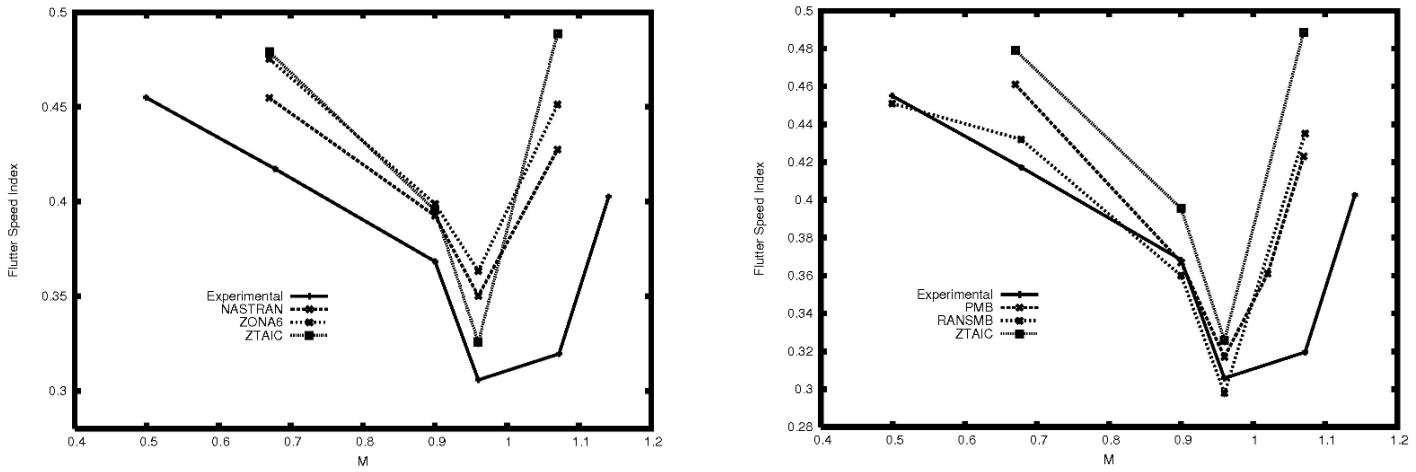
3.0 DESCRIPTION OF LINEAR-BASED METHODS

The aeroelastic analysis has been undertaken using the commercially available NASTRAN and ZAERO packages. Of the various modules available in NASTRAN, it is the DLM (doublet-lattice method) code that is most often used for compressible flow analysis, and hence is most applicable to the transonic analysis considered here (although it should be noted that shock waves are not modelled by this technique, and hence any transonic flow field that contains such is not properly modelled by the DLM). The ZAERO package contains five separate modules for different flow conditions from subsonic to hypersonic. Those used here are ZONA6, based on linear subsonic unsteady aerodynamics, and ZTAIC, a locally linear, but globally non-linear unsteady transonic aerodynamic solver. These methods use a frequency domain approach for flutter calculations, requiring generation of large UAIC (unsteady aerodynamic influence coefficient) matrices to compute the appropriate aerodynamics.

The doublet lattice method (DLM)[12-14] implemented in NASTRAN may be used for the analysis of interfering lifting surfaces and slender bodies of revolution in subsonic flow. It is an extension of the steady vortex-lattice method to unsteady flow, and is based on linearised aerodynamic potential theory. The undisturbed flow is uniform and is either steady or varying harmonically. All lifting surfaces are assumed to lie nearly parallel to the (subsonic) flow. Each of the interfering surfaces is divided into small trapezoidal lifting elements such that the elements are arranged in strips parallel to the free stream with surface edges, fold lines and hinge lines lying on the element boundaries. The unknown lifting pressures are assumed to be concentrated uniformly across the one-quarter chord line of each element. There is one control point per element, centred spanwise on its three-quarter chord line, and the surface downwash boundary condition is satisfied at each of these points. For supersonic flows, another linearised method was used (ZONA51), which has similar assumptions (no thickness effects, small angles, etc.).

The subsonic flow solver ZONA6 implemented in ZAERO differs from the DLM in that it is based on a panel method, and as such may be used to analyse the flow field about the complete aircraft, including interfaces. Thus the aerodynamic effect of the fuselage and/or external stores may be incorporated in a ZAERO analysis. However, in the present analysis of isolated wings, this feature is irrelevant. For supersonic flows, the supersonic variant of the panel method, ZONA7, was used.

https://doi.org/10.1017/S0001924000013208 Published online by Cambridge University Press



(a) Linear (b) General

Figure 1. Flutter boundaries, AGARD 445.6 wing.

ZAERO's ZTAIC module is unique among commercial aeroelastic packages. This module requires external input in the form of steady pressure at various spanwise positions. Zona Technologies states that experimental data is usually preferable, but as this is often unavailable, an alternative approach using input derived from a CFD analysis is possible. In this case the steady surface pressure data was generated by Glasgow University, using the PMB code. This information is used to update the AIC matrix, and allows for a better approximation of the flutter boundary in the transonic flow region.

It is well known that the transonic small disturbance theory may not provide accurate solutions for strong transonic shock cases because it cannot correctly model the entropy gradient from strong shock waves, nor convect the vorticity. However, this is not to say that the transonic small disturbance theory is not suitable for the prediction of unsteady flows due to small aeroelastic deformations if the total unsteady flow is decomposed into a steady background flow and an unsteady component made up of small disturbances. Simplified theories based on the small disturbances approach can yield accurate unsteady flow predictions[15], provided that steady background flow on which the unsteady disturbance propagates is accurately defined.

The ZTAIC method performs an inverse airfoil design that generates an airfoil surface based on the input steady pressure. This is then used to generate the unsteady transonic pressure distribution.

3.1 Intergrid splining

The ZAERO and NASTRAN packages couple the structural and aerodynamic model through a spline matrix (using thin or infinite plate, beam, or rigid body attachment spline methods), that gives all the displacements and slopes in the (x, y, z) directions at all aerodynamic panel control points. The interpolated matrix $\mathbf{G_{as}}$ relates the component of structural grid point deflection $\boldsymbol{\delta}\mathbf{x_s}$ to the deflection of the aerodynamic grid point $\boldsymbol{\delta}\mathbf{x_a}$.

$$\delta x_a = G_{as}\delta x_s \qquad \ldots (16)$$

This transformation ensures structural rather than static equivalence, i.e. the loads produce the same structural displacement. The aerodynamic forces f_a and their structural equivalent values f_s acting on the structural grid points therefore do the same virtual work in their respective deflection modes

$$(\delta x_a)_V^T f_a = (\delta x_s)_V^T f_s \qquad \ldots (17)$$

where $(\delta\mathbf{x_a})V$ and $(\delta\mathbf{x_s})$V are virtual deflections. Substituting Equation (13) into the left-hand side of Equation (14) and rearranging yields

$$(\delta x_s)_V^T \left(G_{as}^T f_a - f_s\right) = 0 \qquad \ldots (18)$$

from which the required force transformation

$$f_s = G_{as}^T f_a \qquad \ldots (19)$$

is obtained because of the arbitrariness of the virtual deflections. Equations (13) and (16) are both required to complete the formulation of aeroelastic problems in which the aerodynamic and structural grid points do not coincide.

4.0 DYNAMIC TEST CASES

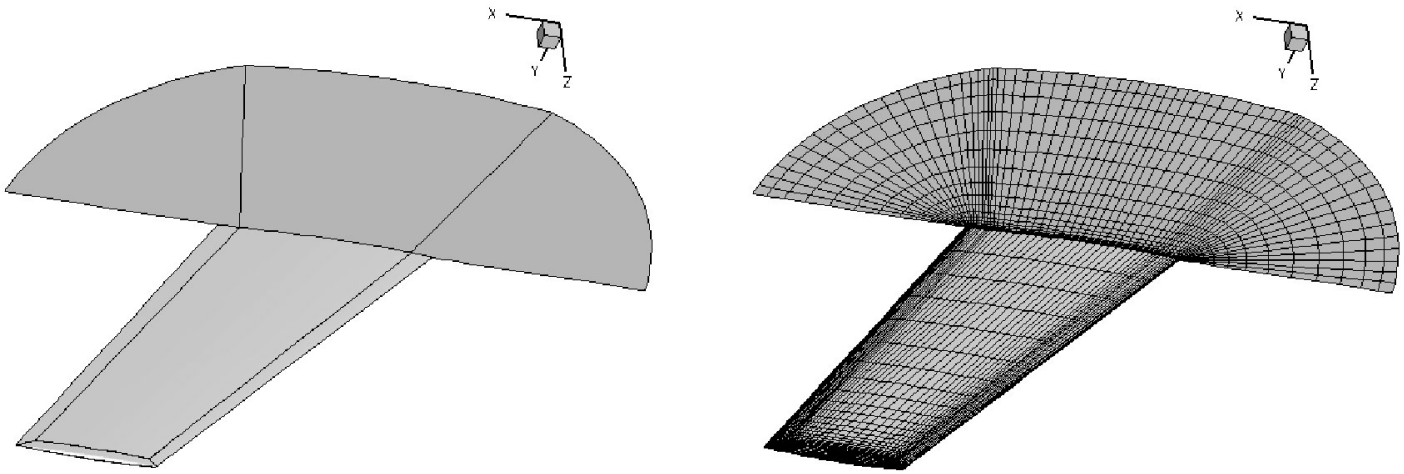
4.1 AGARD 445.6 weakened wing

The AGARD 445.6 wing was constructed of mahogany with a 45° quarter chord sweep, a root chord of 22·96in, and a constant NACA64A004 symmetric profile[16]. A series of flutter tests, carried out at the NASA Langley Transonic Dynamics Tunnel to determine stability characteristics, were reported in 1963. Of the various wing models tested, the most published results appear for the weakened wing (wing 3) in air. This wing had holes drilled out and filled with plastic to reduce stiffness whilst maintaining aerodynamic shape. Published experimental data includes the flutter boundary for several Mach numbers in the range 0·338 to 1·141. The structural characteristics of the wing were provided in the form of measured natural frequencies and mode shapes derived from a finite element model.

The wing has been the subject of many previous studies, using linear[17], linear plus non-linear corrections[18], TSD[19], TSD plus boundary layer[20], and structured and unstructured Euler and Navier Stokes CFD[21-25] methods. Generally, it was found that the TSD results were less accurate than linear methods, that the CFD techniques were superior overall, but were poor in the supersonic region, and that grid refinement remained an issue. Viscosity and mode number in the structural model were found to have an effect, but the magnitude of this depended on Mach number.

A comparison of the flutter boundaries produced by the methods under investigation is shown in Figs 1(a) and 1(b). For the results

https://doi.org/10.1017/S0001924000013208 Published online by Cambridge University Press



(a) (b)

Figure 2. Grid topology (left) and medium surface mesh (right).
Note that only the inner blocks above the wing are shown on the symmetry plane.

presented here, the structural grid contained ten chordwise, and 20 spanwise elements, equidistantly spaced in span and local chord. The effect of structural grid density and mode number was investigated in the wider project, and found generally to have little effect[26] (there were, however, some exceptions to this rule, see the full report for details). The same grid was used for both structural and aerodynamic purposes in the linear codes.

Several aerodynamic grids were generated for use with PMB and RANSMB, of CH and O type and surface node numbers varying between 1,100 and 18,000. Figure 2 shows the O topology and a typical grid. An investigation of mesh density found convergence of flutter speed prediction was improved if cells were clustered towards the outer span. More details are available in Ref. 26, the discussion which follows is based on the complete set of results.

The flutter boundaries predicted by the linear methods (Fig. 1(a)), produce the correct overall trends, and demonstrate a reduction in flutter speed index with increasing Mach number, reaching a minima at about the same Mach number as the experimental results. As the linear methods cannot allow for the effects of transonic regions, the clear implication is that this behaviour is solely due to the effects of compressibility. However, the flutter speed is predicted on average about 10% too high. The methods reliant on purely linear aerodynamics (labelled NASTRAN and ZONA6) produce very similar boundaries, although the NASTRAN results are generally 2 or 3% lower (and hence nearer the experimental boundary) across all speeds. It should be noted here, however, that the aerodynamic model associated with these solution methods is fundamentally incapable of accurately representing the flow field surrounding the wing, either statically of dynamically in the transonic region. The results produced should therefore be treated with some caution.

As stated previously, the ZTAIC method is globally non-linear, due to the CFD derived steady flow field used as input. However, the unsteady aerodynamic formulation assumes small perturbations from one dimensional flow, and as such represents an approximation of the dynamic situation. It may be considered to represent an intermediate method between the rapid, but physically questionable linear methods, and the more time consuming, but physically correct (at least within the context of an inviscid flow) coupled codes. It is therefore interesting to note that in general, the flutter boundary estimated is very close to that of ZONA6 in the subsonic region, but produces a more pronounced minima in flutter speed index in the dip, closer to the experimental value than either of the other two codes, and similar to that the code from which the pressure inputs were derived (PMB).

The results for the more advanced non-linear codes are given in Fig. 1(b). Agreement between RANSMB and PMB is good, as would be expected given the similarity of the methods, although RANSMB consistently predicts a slightly lower flutter speed than PMB. The correlation of the flutter boundary with experiment is improved over that demonstrated by the linear methods, even in the low speed regime, and particularly so in the transonic dip. Although significant errors (compared to experiment) are present in supersonic flow, this is consistent with other results using similar methods[25,27].

Taking all these results into consideration, it would seem, therefore, that the error associated with the use of a linearised aerodynamic model may be broken in to two parts; that due to the limitations of the equations solved generally, and that related to the effects of transonic flows. The unsteady coefficients in both ZAERO solutions (ZONA6 and ZTAIC) and NASTRAN's DLM are produced by solving the unsteady small disturbance equation — this requires the assumption of a primary flow in a purely chordwise direction, and hence is of limited accuracy near the leading and trailing edges, and cannot properly allow for the effects of sweep. There is therefore an error in flutter speed index produced across the full Mach number range. In the transonic region, an extra error is produced by the lack of modelling the effects of shock waves, which (at least in the case of inviscid flow) produce an exaggeration of the effects of compressibility, and hence a greater reduction in flutter speed index. This latter effect is, at least partially, allowed for in the ZTAIC method by the use of a non-linear CFD derived flow field as input.

4.2 The MDO wing

The AGARD wing is symmetric and extremely thin, design features which increase the applicability of the linearised methods discussed, but reduce similarity with practical designs for transonic aircraft. In order to gauge the performance of the techniques discussed on a more realistic design, a second case was examined, this being the MDO wing. This presents a more serious challenge to the linear methods, as the neglected aerofoil thickness plays a crucial role in aeroelastic behaviour.

The multi-disciplinary optimisation (MDO) wing was extracted from the MDO aircraft designed in a Brite-Euram project to establish design methodology for future large commercial aircraft.

It was used in the unsteady flow in the context of fluid-structure interaction (UNSI) project as a test case for coupled CFD-structural dynamics simulations. Comparison of the results between the

https://doi.org/10.1017/S0001924000013208 Published online by Cambridge University Press

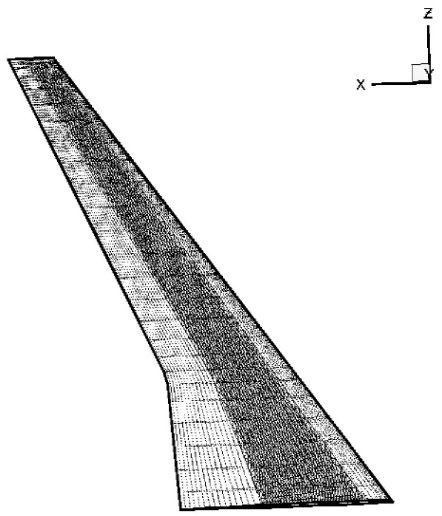


Figure 3. MDO wing planform.
The dark shaded region indicates the extent of the structural model.

different partners can be found in various publications of the UNSI group[27-29]. The MDO configuration was optimised for high performance at a particular cruise condition. The optimising calculations were started from an estimate of the jig shape which leads to the design shape at cruise conditions. The wing has a semi-span of 36m, a thick supercritical section, and a planform as shown in Fig. 3.

The UNSI partners involved in the comparison of the coupled CFD-CSD analyses of the MDO wing were Alenia, BAE Systems, Dassault, ONERA, and Saab. A total of eight different solution methods were used, including a fully coupled Euler-NASTRAN analysis, and Euler, viscous full potential, and transonic perturbation schemes coupled to modal analysis. Static and dynamic test cases were devised, and the results produced showed some notable differences even between similar methods, without identifying the specific cause[27,29]. Possible explanations included the accuracy with which the CFD scheme calculates the loading, the effectiveness and consistency of the load transfer algorithm, the accuracy of the structural calculation, and the accuracy with which the displacement algorithm transforms the aerodynamic shape (Ref. 29, page 318). The interpolation methods used were IPS (infinite plate spline) or polynomial methods for ONERA, interpolation on an intermediate grid for Dassault and the use of rigid elements in the NASTRAN solver by Alenia.

Three test cases were used for the comparisons and are summarised in Table 1. An extra case (4) was devised specifically for the current work at a Mach Number of 0·3 to allow comparison with linear methods employed away from the non-linear transonic region. In all respects except Mach number (and hence velocity) conditions were the same as in Case 1. For each code the angle of attack was chosen to match the design lift coefficient.

Table 1
Conditions for MDO test case

	Case 1	Case 2	Case 3	Case 4
Mach number	0·85	0·88	0·88	0·3
Lift coefficient	0·4581	0·3263	0·1686	0·4581
Aircraft mass	371 tons	537 tons	537 tons	–
Altitude	11·27km	7km	2km	11·27km

The lift coefficient quoted here is scaled in terms of the wing surface area, 725m²

Comparison of the methods developed under the PUMA DARP is made with Saab and ONERA codes, which are representative of the results from the UNSI study, and involve methodologies most similar to that of the coupled codes described here[28].

The Saab results were generated using the EURANUS code, which solves on multiblock structured grids using explicit time stepping and multigrid. Central and upwind differencing options are available. The mesh is moved via a sequence of pre-determined perturbation grids (in this case based on 18 modes). The transfer is achieved by projection onto a neutral surface and interpolation to obtain the displacement of projected points. Pseudo-time stepping is used for unsteady calculations and pseudo iterations are used to remove sequencing effects between the fluid and structural solutions.

ONERA's CANARI code is a structured cell-centred Euler solver, and was coupled to a NASTRAN derived 20 mode structural model to define structural motion for the transpiration based aerodynamic-structure interface. The ONERA aerodynamic grid contained 365541 nodes, and the SAAB grid 106425.

4.2.1 Selected results

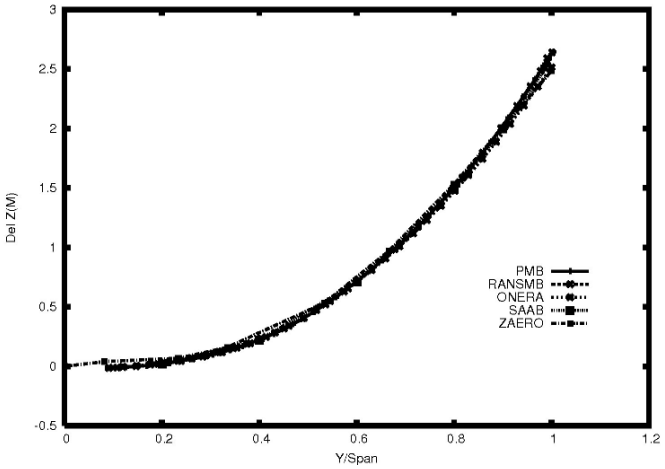
A subset of a large database of results are presented herein; the conclusions are based on the complete set. As the aerodynamic mesh density used by RANMSB and PMB could only match either that of SAAB or ONERA, the smaller SAAB mesh was used to reduce calculation time. In all results presented here for the coupled codes, the wing was structurally modelled as a box using finite elements, and the first 18 of the resulting mode shapes were used in the calculations. The static results were produced through simulation of the artificially damped wing under the conditions prescribed, the flutter boundaries calculated by removing the damping and disturbing the wing from the steady state.

Results generated by the use of the commercial packages were produced using a common structural/aerodynamic grid, split into three sections, the root, containing three spanwise and 13 chordwise elements, an inner wing section extending to the kink in the planform containing 11 by 13 elements, and from the kink to the tip also containing 11 by 13 elements. Mesh refinement was studied, but found to make little difference to the solution[26].

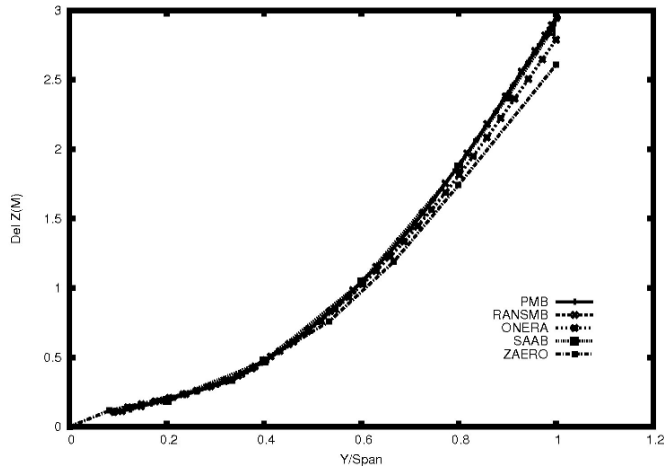
Although flutter calculations are the primary focus of this paper, a brief examination of the static cases is presented. This is done primarily because of the aforementioned discrepancy between other non-linear calculations, in an attempt to determine which of the four factors identified is responsible. This question is itself of importance; ACARI 2020 specifications for new aircraft require a significant reduction in fuel burn. One straightforward way in achieving a portion of this reduction is to reduce the mass of the vehicle. However, this will inevitably result in a more flexible aircraft, and this in turn will not only require a reliable simulation/prediction capability for dynamic interactions, but also increase the need for accurate determination of the position of, and pressure distribution around, deformed wings. There is, after all, no point in carefully optimising a wing shape for minimising drag if, due to the flexibility of the structure, that particular wing position never actually occurs in flight. Results derived from a ZAERO (ZONA6) analysis are also included, to provide a comparison of the performance of current commercial linear-based methods with the more advanced (but time intensive) time marching solutions. Comparison should be viewed with some care, however, as the effects of camber were not included, due to a number of timing issues. The formulation of ZAERO does allow these effects to be modelled, and would improve the results.

Typical of the static results were those produced under Case 1 conditions. This required a lift coefficient of 0·4581 under conditions as specified in Table 1, achieved with an incidence of 1·148° using PMB, and 0·931° with RANSMB. This compares to 0·745 and 0·8925° for the same case generated by Saab and ONERA codes.

https://doi.org/10.1017/S0001924000013208 Published online by Cambridge University Press



(a) Leading edge

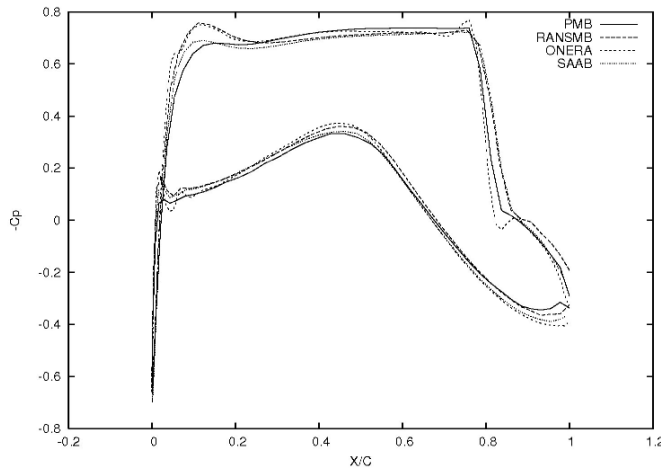


(b) Trailing edge

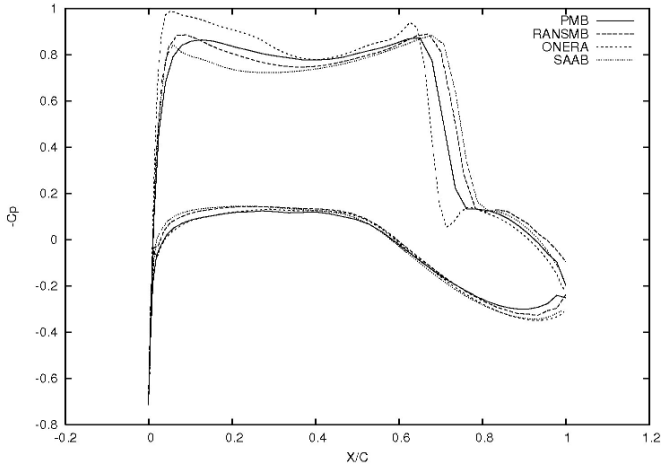
Figure 4. Leading and trailing edge deflections, MDO Wing, Case 1.

The linear method (ZAERO), however, requires an incidence of 5·3°. The leading and trailing edge displacements produced are shown in Fig. 4. Excellent agreement between RANSMB and PMB is demonstrated, with good agreement with the other two coupled codes. The ZAERO displacements also show good correlation, despite the much higher incidence. This is because the test cases require a force balance, and hence total force required is similar for all methods, producing roughly equivalent deflections.

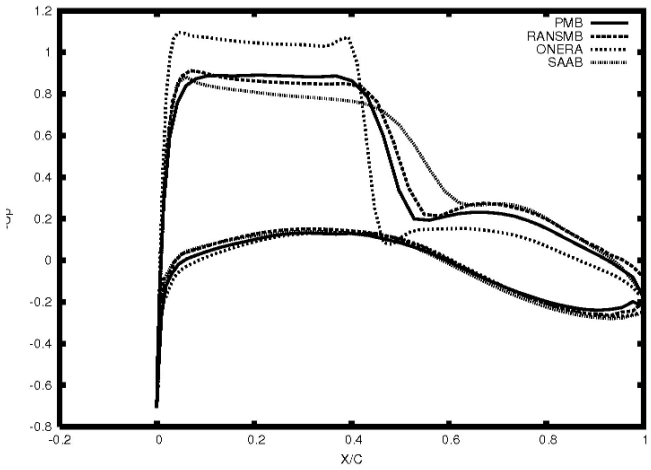
Figure 5 shows the pressure distributions at 20, 60, and 90% of the span produced by the non-linear methods. Generally, agreement between the RANSMB and PMB solutions is notably better than that between Saab and ONERA, and pressures predicted using RANSMB and PMB lie between the predicted pressures of the SAAB and ONERA codes. This includes the 90% span section, where deflections were substantial (in some cases about 10% of the semi-span). This may be due to the better agreement in deflection in this region, as well as more accurate interpolation of aerodynamic grid. Near the root region, however, the pressures about the leading edge predicted by RANSMB match ONERA results more closely, whilst those of PMB are more similar to Saab. This implies that these differences are largely due to the differencing formulation (central differencing vs. upwinding), although it should be noted that the ONERA results were based on a finer grid than the other three (containing around 300,000 points as opposed to about 100,000). The discrepancy in pressure between PMB and RANSMB at the root is likely to be a



(a) 20% span



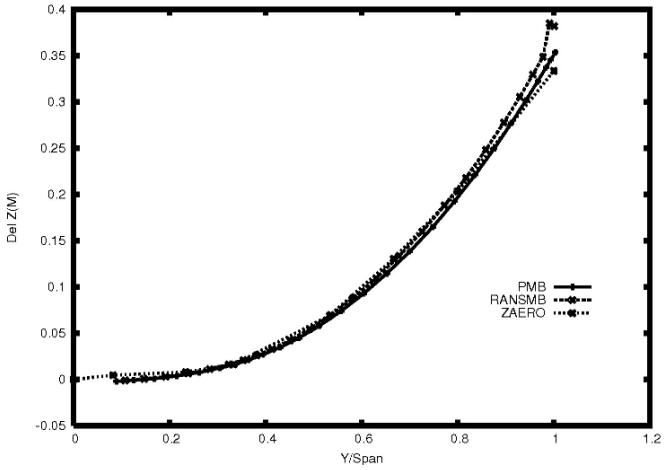
(b) 60% span



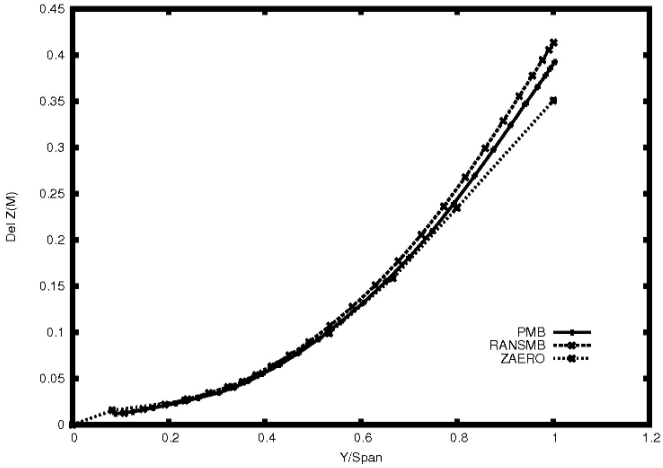
(c) 90% span

Figure 5. Pressure distributions, MDO Wing, Case1.

https://doi.org/10.1017/S0001924000013208 Published online by Cambridge University Press

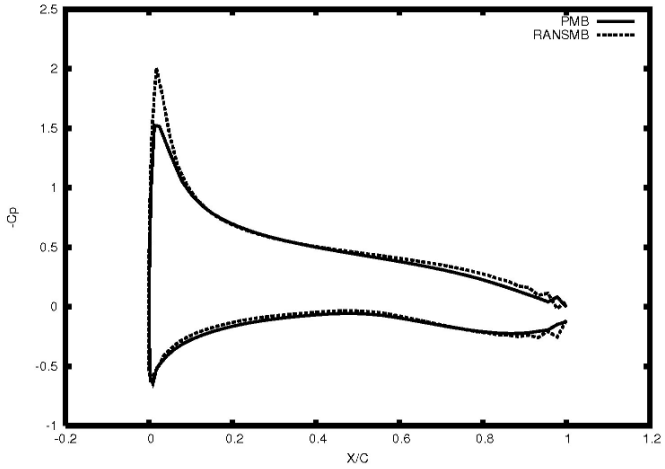


(a) Leading edge

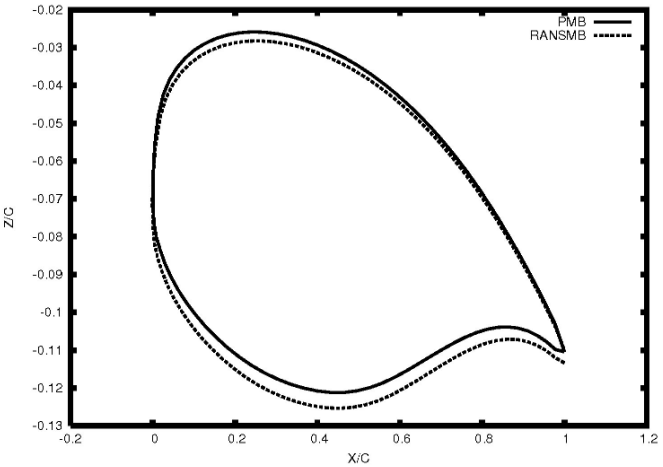


(b) Trailing edge

Figure 6. Leading and trailing edge deflections, MDO Wing, Case 4.



(a) pressure distribution



(b) Aerofoil sections

Figure 7. The 80% span section, MDO Wing, Case 4.

part of the reason for the difference in incidence needed to achieve the required lift coefficient. However, it is also notable that the shock wave position in the RANSMB solution is always slightly rearwards of that produced by PMB, and hence also results in a slightly greater lift for a given incidence. Results from Cases 2 and 3 produced similar trends.

Case 4 differs from the other cases in that it has not previously been examined by other workers. Its primary function is to allow comparison of linear and non-linear methods within the subsonic regime, where linear methods would be expected to produce accurate results. The conditions were maintained identical to Case 1, except that the Mach number (and hence velocity) was lowered to 0·3 (88·5ms^{-1}).

The cell-centred method (RANSMB) again predicts a higher suction peak at a given incidence, and this feature is more noticeable for this subsonic case. This means that the required lift coefficient of 0·4581 is achieved at only 1·60°, somewhat lower than the 2·37° required for PMB, and considerably lower than the 4·21° predicted by ZAERO. Despite this, the coupled codes maintain very good agreement in terms of deflection, pressure distribution, and aerofoil section (see for example Figs 6 and 7). The deflection predicted by the linear ZTAIC method is again similar.

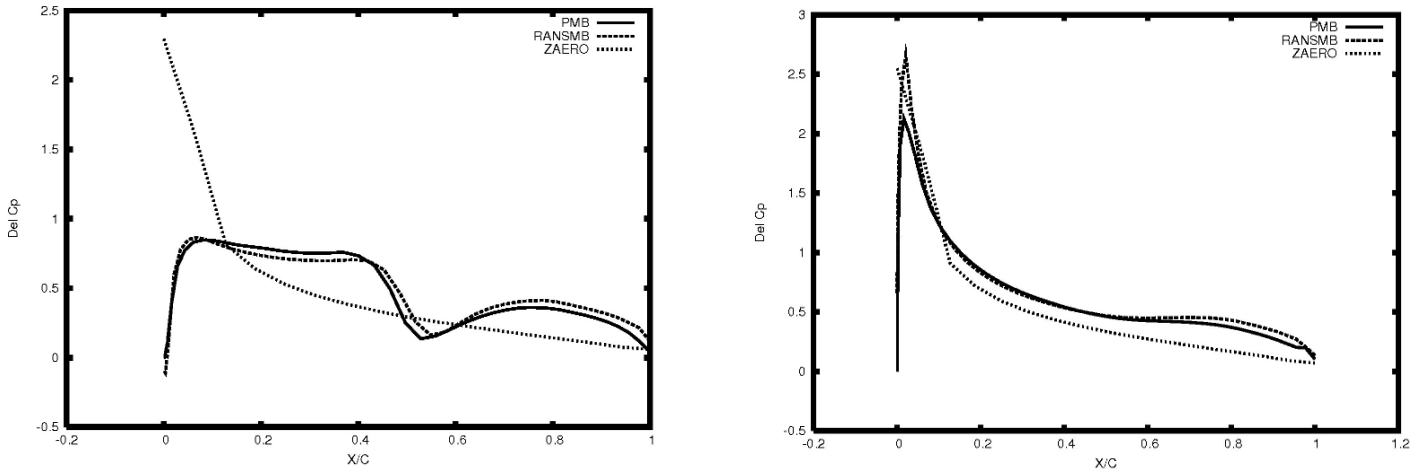
The difference between upper and lower surface pressure coefficients is shown for the 90% span section in Fig. 8 for Case 1 and 4. The tendency for the linear method to under predict the lift generated on the rear of the aerofoil is increased in the transonic regime. This explains the more similar incidence required for Case 4 (only about twice the non-linear codes, as opposed to over five for Case 1).

4.2.2 Summary of trends

The results presented here and elsewhere[26] allow the following conclusions to be drawn:

- Agreement between PMB and RANSMB in terms of pressure distributions and deformations is generally excellent. This in turn implies that flow solver methodology (upwind *vs* cell centred) has less effect on coupled calculations than the interpolation and grid motion methods. The exception to this is the leading edge pressures near the root, where solver methodology (cell centred vs. upwind) is the principle factor, cell-centred codes producing a higher suction. This is likely to be related to the relatively coarse grid used for these calculations (only 81 × 26 points on the surface of a fairly complex wing geometry). An examination of grid dependence is therefore underway.

https://doi.org/10.1017/S0001924000013208 Published online by Cambridge University Press



(a) Case 1 (b) Case 4

Figure 8. Pressure differences, MDO Wing, Case 1 and 4, 90% Span.

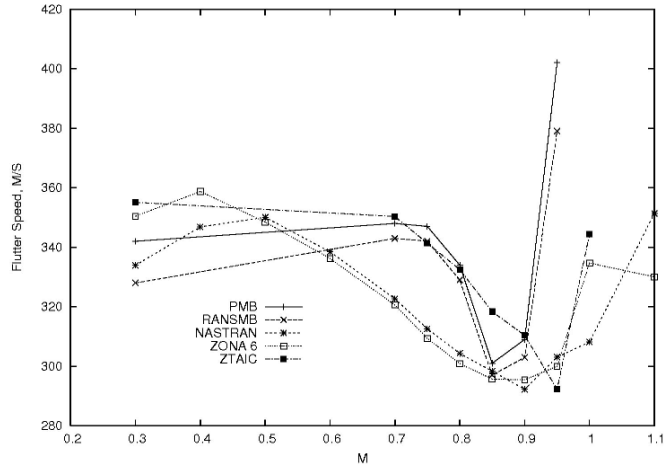


Figure 9. Flutter boundaries, $\alpha = 0°$, $\rho = 1.006 kgm^{-3}$

- The linear method (ZAERO) tends to require higher incidences to generate the required lift. The neglect of camber effects no doubt contribute to this, but examination of the pressure distributions reveals that this is also due in part to a failure to predict the lift generated over the rear of the aerofoil, leading to an increased incidence, and thus a higher suction peak at the leading edge. This effect is intensified in the transonic region due to the rooftop design, and presence of shock waves. The incorrect chordwise lift distribution also induces a greater twist along the span. The deflections caused by the loading, however, are similar to those produced by the non-linear methods, as the total forces acting on the structural models is the same.

4.2.3 Flutter boundary

The flutter boundaries of the MDO wing predicted by the various linear and non-linear codes under investigation are shown in Fig. 9. The flutter speed assumes an atmospheric density of $1{\cdot}006 kgm^{-3}$, and calculations were carried out at zero incidence.

Agreement between PMB and RANSMB is generally very good. As was the case with the AGARD 445.6 wing, RANSMB consistently predicts a lower flutter speed than PMB, but the difference is small over the majority of the Mach number range (about 1%). It is probable that this is caused by the previously noted tendency of RANSMB to predict higher suction at the leading edge for a given angle of incidence. Under small oscillations about a nominal angle of attack, this will tend to destabilise the motion more rapidly, and hence produce a lower flutter boundary. This would also explain the greater discrepancy at the lowest Mach number (M = 0·3), as it was noted previously that this effect was greatest at these conditions.

Whilst no experimental data exists for comparison, the formulation of the methods, similarity of the RANSMB and PMB results, and AGARD 445.6 wing results suggest that the true behaviour of the MDO wing would be closer to that predicted by the non-linear methods, at least up to the 'floor' of the dip (~Mach 0.9). It is likely that, as for the AGARD445.6, the flutter speed is considerably over predicted at Mach numbers higher than this.

The flutter boundary predicted by NASTRAN'S DLM/ZONA51 and ZAERO ZONA6 are again generally very similar (up to M = 0·95), as might be expected from the similarity of their formulation. However, the agreement of these methods does not necessarily imply accuracy. If the conclusion of the previous paragraph is granted, then it may be seen that the effects of compressibility on the wing are over-estimated, with a drop in flutter speed index in evidence at much lower Mach numbers than that predicted by the time marching codes. It is true that the minimum flutter speed predicted by all the commercial codes is very close to that of the non-linear methods, but the dissimilarity of surrounding results suggest this may be coincidental. It is again worth emphasising that at any speed at which a transonic flow exists, the governing equations of the linearised methods are incapable of correctly representing the flow, and thus the results produced must be viewed with caution. This is obviously a more severe limitation with the MDO wing than for the AGARD, as the relative thickness of the wing means that such regions will form at lower Mach numbers.

As was the case with the AGARD445.6 wing, the predictions produced by the standard linear tools may be improved by including non-linear effects in the steady state formulation (as shown by the flutter boundary predicted using ZTAIC), but this in itself does not appear to be sufficient to match the performance of the fully non-linear aerodynamic methods.

Whilst potentially more accurate, the run time required by the non-linear methods to predict the flutter boundary is considerably greater than the alternative techniques. It is also dependent upon a

https://doi.org/10.1017/S0001924000013208 Published online by Cambridge University Press

number of factors, which do not affect the linear methods. This is due to the time-marching nature of the former, as opposed to the frequency domain analysis of the latter. These factors include time step and period of simulation (smaller time steps and longer periods increase accuracy but also increase run time), the allowable maximum velocity gap between a stable and unstable condition (determined by the nature of the flutter boundary crossing), and whether a rough location of the position of the flutter boundary is already known. The first two factors effect the length of time any given calculation takes, the second two the number of such calculations required to accurately locate the boundary. However, as a rough rule of thumb, for each point on the MDO flutter boundary NASTRAN calculations took of the order of a minute, ZAERO about 20 to 30 times this, and the non-linear techniques a further factor of 30 to a 100, depending upon the aforementioned factors. It is assumed that the set up time for the problems is irrelevant — the structural and aerodynamic models needed for all of the solution methods described are assumed to be extant due to other drivers in the design cycle (e.g. an aerodynamic grid suitable for CFD analysis will already have been created to allow estimation of aerodynamic performance in the steady state, etc.).

5.0 CONCLUSIONS

The analysis of the AGARD 445.6 wing demonstrates that the linear methods may be used to achieve a reasonable estimation of the flutter boundary of a wing if it is of simple design. Even here, however, the coupled Euler-modal methods were demonstrated to produce results more similar to experiment.

Analysis of the results for the MDO wing reveals that PMB and RANSMB perform in a very similar manner, despite using different solver methodologies (upwind *vs* central differencing). This in turn implies that the reason for the differing results found in previous studies are primarily due to the interpolation between the structural and aerodynamic grids. The only notable differences between RANSMB and PMB solutions appear to be caused by the relatively coarse nature of the grid near the leading and trailing edges. This point is deemed significant, as two independent codes have for the first time generated excellent agreement for this dynamic aeroelastic test case, and the implication may be drawn from this that the key factor in aeroelastic simulations, that of accurately linking the structural motion and the aerodynamic surface grid, has been achieved. However, it must be acknowledged that this is based on the results from only two test cases, one of which is entirely computational. This leads to the conclusion that the lack of a realistic dynamic test case based on experiment in the open literature is a serious impediment to the development, and particularly verification, of advanced aeroelastic formulations.

The comparison of the commercial linearised codes with the time marching methods has demonstrated both the strengths and weaknesses of the former. A much more rapid solution is obtainable, but accuracy must be sacrificed, particularly at higher Mach numbers. Although an intermediate methodology based on updating the linear solution with non-linear steady state pressure distribution goes some way to remedying this, due to the limitations associated with small disturbance solutions, this cannot in itself resolve the problems in their entirety. Furthermore, any phenomena which involves larger scale motions (e.g. LCO prediction, etc.) cannot be modelled as a small disturbance (although flutter results in such large scale motion, flutter onset is essentially an infinitesimal motion, and hence can be represented in this manner). However, the time scales required for solution with time marching solutions are effectively prohibitive within the initial design stage (although this is not necessarily a problem if the codes are to be used in conjunction with a flight test programme in an effort to reduce the cost of the latter). It is therefore apparent that some alternative technique, offering calculations of comparable time scales to the linear methods, but formulated in a manner to allow the retention of the true non-linear nature of the flow field, would be a highly desirable. It is with such methods that the aeroelastics group of the PUMA DARP is now concerned.

ACKNOWLEDGEMENTS

This work has been carried out under the PUMA DARP's 2002 programme: financial support from EPSRC, MoD, DTi, Airbus and BAE Systems is acknowledged. The authors are grateful to both academic and industrial members of the PUMA aeroelastics Focus Group for their assistance.

REFERENCES

1. OSHER, S. and CHARKRAVARTHY, S. Upwind schemes and boundary conditions with applications to Euler equations in general geometries, *J Computational Physics*, 1983, **50**, pp 447-481.
2. VAN LEER, B. Towards the ultimate conservative difference scheme II: Monotonicity and conservation combined in a second order scheme, *J Computational Physics*, 1974, **14**, pp 361-374.
3. JAMESON, A. Time dependent calculations using multigrid, with applications to unsteady flows past airfoils and wings, AIAA Paper 91-1596.
4. SCHMIDT, W., JAMESON, A. and TURKEL, E. Numerical solutions of the euler equations by finite volume methods using Runge-Kutta time stepping schemes, 1981, AIAA-Paper 81-1259.
5. GAITONDE, A.L. A dual-time method for the solution of the unsteady euler equations, *Aeronaut J*, October 1994, **98**, 978, pp 283-291.
6. MELSON, N.D., SANETRIK, M.D. and ATKINS, H.L. Time-accurate Navier-Stokes calculations with multigrid acceleration, 1993, Technical Report CP 3224, NASA.
7. GERADIN, M. and RIXEN, D. *Mechanical Vibrations*, Second edition, 1997, John Wiley and Sons, Chichester, UK.
8. BATHE, K.J. *Finite Element Procedures in Engineering Analysis*, 1982, Prentice Hall, Englewood Cliffs, NJ, USA.
9. GOURA, G.S.L. Time Marching Analysis of Flutter using Computational Fluid Dynamics, 2001, PhD thesis, Department of Aerospace Engineering, Glasgow University.
10. JONES, D.P. Force transfer in aeroelastic calculations, December 2002, Technical Report AE047, University of Bristol.
11. GORDON, W.J. and HALL, C.A. Construction of curvilinear co-ordinates systems and applications to mesh generation, *Int J for Numerical Methods in Engineering*, 1973, **7**, pp 461-477.
12. ALBANO, E. and RODDEN, W.P. A doublet-lattice method for calculating lift distributions on oscillating surfaces in subsonic flows, *AIAA J*, 1969, **7**, pp 179-285.
13. GIESING, J.P., KALMAN, T.P. and RODDEN, W.P. Subsonic unsteady aerodynamics for general configurations; Part I, Vol I — direct application of the nonplanar doublet-lattice method, 1971, Technical Report AFFDL-TR-71-5, Part I, Vol I, Airforce Flight Dynamics Laboratory.
14. RODDEN, W.P., GIESING, J.P. and KALMAN, T.P. Refinements of the nonplanar aspects of the subsonic double-lattice lifting surface method, *J Aircr*, 1972, **9**, pp 69-73.
15. LIU, D.D. KAO, Y.F. and FUNG, K.Y. An efficient method for computing unsteady transonic aerodynamics of swept wings with control surfaces, *J Aircraft*, 1988, **52**, (1), pp 25-31.
16. YATES, E.C. Standard aeroelastic configurations for dynamic response I — wing 445.6, September 1985, Technical Report 765, AGARD. Includes Tech Report TN-D-1616 as an Appendix.
17. *Version 3.2. ZAERO Applications Manual*, Zona Technology, Arizona.
18. DA SILVA, R.G.A and DE FARIA MELLO, O.A. Prediction of transonic flutter using Nastran with aerodynamic coefficients tuned to Navier Stokes computations, 1999, CEAS/AIAA/ICASE/NASA meeting on Aeroelasticity and Structural Dynamics, June 1999, Norfolk,VA, USA.
19. BATINA, J.T., BENNETT, R.M., SEIDEL, D.A., CUNNINGHAM, H.J. and BLAND, S. Recent advances in transonic computational aeroelasticity, *Computers and Fluids*, 1998, **30**, (172), pp 29-37.
20. EDWARDS, J.T. Calculated viscous and scale effects on transonic aeroelasticity, 1997, AGARD SMP meeting on Numerical Unsteady Aerodynamic and Aeroelastic Simulation, Aalborg, Denmark, Published in AGARD R-822, October 1997.
21. GUPTA, K.K. Development of a finite element aeroelastic analysis capability, *J Aircr*, 1996, **33**, (5), pp 995-1002.

https://doi.org/10.1017/S0001924000013208 Published online by Cambridge University Press

22. MELVILLE, R.B., MORTON, S.A and RIZZETTA, D.P. Implementation of fully-implicit aeroelastic Navier-Stokes solver, 1997, 13th Computational Fluid Dynamics Conference, 29 June-2 July 1997, Snowmass Village, CO, USA, AIAA paper 97-2039, 1997.
23. RAUSCH, R.D., BATINA, J.T, and YANG, H.T. Three-dimensional time-marching aeroelastic analyses using an unstructured-grid Euler method. *AIAA J*, 1993, **31**, (9), pp 1626-1633.
24. LESONNE, M. and FARHAT, C. High order subiteration-free staggered algorithm for nonlinear transient aeroelastic problems. *AIAA J*, 1998, **36**, (9), pp 1754-1757.
25. GORDNIER, R.E. and MELVILLE, R.B. Transonic flutter simulations using an implicit aeroelastic solver, *J Aircr*, 2000, **37**, (5), pp 872-879.
26. TAYLOR, N.V., JONES, D.P., GAITONDE, A., ALLEN, C.B., BADCOCK, K.J., WOODGATE, M.A., RAMPURAWAL, A.M., COOPER, J.E. and VIO, G.A. Evaluation of the influence of aerodynamic modelling on the transonic aeroelastic prediction of three wing test cases, October 2004, Technical report, PUMA DARP.
27. GIRODOUX-LAVIGNE, P., GRISVAL, J.P., GUILLEMOT, S., HENSHAW, M., KARLSSON, A., SELMIN, V., SMITH, J., TEUPOOTAHITI, E. and WINZELL, B. Comparison of static and dynamic fluid-structure interaction solutions in the case of a highly flexible modern transport aircraft win, *J Aero Sci and Tech*, 2003, **7**, pp 121-133.
28. GIRODOUX-LAVIGNE, P., GRISVAL, J.P., GUILLEMOT, S., HENSHAW, M., KARLSSON, A., SELMIN, V., SMITH, J., TEUPOOTAHITI, E. and WINZELL, B. Comparative study of advanced fluid-structure interaction methods in the case of a highly flexible wing, 2001, Results from the UNSI program, International Forum Aeroelasticity Structural Dynamics, June 2001, Madrid.
29. HAASE, W., SELMIN, V. and WINZELL, B. (EDS). *Progress in Computational Flow-Structure Interaction*, 2003, Vol 81 of Notes on Numerical Fluid Mechanics and Multidisciplinary Design, Springer-Verlag.

https://doi.org/10.1017/S0001924000013208 Published online by Cambridge University Press